Journal of Crystal Growth 350 (2012) 80–84

Contents lists available at SciVerse ScienceDirect

Journal of Crystal Growth

journal homepage: www.elsevier.com/locate/jcrysgro

Zinc-blende and wurtzite $Al_xGa_{1-x}N$ bulk crystals grown by molecular beam epitaxy

S.V. Novikov [a,*], C.R. Staddon [a], F. Luckert [b], P.R. Edwards [b], R.W. Martin [b], A.J. Kent [a], C.T. Foxon [a]

[a] School of Physics and Astronomy, University of Nottingham, Nottingham NG7 2RD, UK
[b] Department of Physics, SUPA, University of Strathclyde, Glasgow, G4 0NG, UK

ARTICLE INFO

Available online 13 December 2011

Keywords:
A1. Substrates
A3. Molecular beam epitaxy
B1. Nitrides
B2. Semiconducting III-V materials

ABSTRACT

There is a significant difference in the lattice parameters of GaN and AlN and for many device applications $Al_xGa_{1-x}N$ substrates would be preferable to either GaN or AlN. We have studied the growth of free-standing zinc-blende and wurtzite $Al_xGa_{1-x}N$ bulk crystals by plasma-assisted molecular beam epitaxy (PA-MBE). Thick (~10 μm) zinc-blende and wurtzite $Al_xGa_{1-x}N$ films were grown by PA-MBE on 2-in. GaAs (0 0 1) and GaAs (1 1 1)B substrates respectively and were removed from the GaAs substrate after the growth. We demonstrate that free-standing zinc-blende and wurtzite $Al_xGa_{1-x}N$ wafers can be achieved by PA-MBE for a wide range of Al compositions.

1. Introduction

Currently there is high level of interest in the development of ultraviolet (UV) light sources for solid-state lighting, optical sensors, surface decontamination and water purification. III-V semiconductor UV LEDs are now successfully manufactured using the $Al_xGa_{1-x}N$ material system, covering the energy range from 3.4 eV (GaN) up to 6.2 eV (AlN). The majority of UV LEDs require $Al_xGa_{1-x}N$ layers with compositions in the mid-range between AlN and GaN. For example for efficient water purification such $Al_xGa_{1-x}N$ LEDs need to emit in the wavelength range 250–280 nm. However, there is a significant difference in the lattice parameters of GaN (a~3.19 Å and c~5.19 Å) and AlN (a~3.11 Å and c~4.98 Å) [1]. Therefore $Al_xGa_{1-x}N$ substrates would be preferable to those of either GaN or AlN for many ultraviolet device applications, which require active $Al_xGa_{1-x}N$ layers with x~0.5. That has stimulated the current active search for methods to produce bulk $Al_xGa_{1-x}N$ substrates with variable AlN content.

The group III-nitrides normally crystallise in the wurtzite structure, which has a hexagonal symmetry. High quality bulk wurtzite (hexagonal) GaN substrates can be grown from liquid Ga solutions. However, the solubility of N in liquid Ga is very low and it is difficult to obtain reasonable growth rates. It is possible to increase the N solubility in Ga by using high pressures and high temperatures [2]. There are a few reports in the literature on the growth of bulk $Al_xGa_{1-x}N$ crystals using Ga melt solutions under high nitrogen pressure and at high temperatures [3,4]. However, the size of bulk $Al_xGa_{1-x}N$ crystals currently achieved by that method is still very small (up to ~$0.8 \times 0.8 \times 0.8$ mm^3) [4].

Several companies are now offering free-standing bulk wurtzite GaN substrates grown by MOVPE or HVPE. These are thick GaN layers grown on different non-nitride substrates and after that separated from the substrate. The size of commercially available bulk hexagonal GaN substrates has reached 2-in. diameter and thicknesses up to 0.5 mm. There are now attempts to grow free-standing wurtzite $Al_xGa_{1-x}N$ bulk crystals with different compositions by metal-organic vapour phase epitaxy (MOVPE) or hydride vapour phase epitaxy (HVPE) [5]. However, to the best of our knowledge, so far there was only one conference report several years ago on the growth of free-standing wurtzite $Al_xGa_{1-x}N$ bulk layers with a thickness up to 0.6 mm by HVPE [6].

Molecular beam epitaxy (MBE) is normally regarded as an epitaxial technique for the growth of very thin layers with monolayer control of their thickness. However, we have recently successfully used the plasma-assisted molecular beam epitaxy (PA-MBE) technique for bulk crystal growth and we produced free-standing layers of metastable zinc-blende (cubic) GaN up to 100 μm in thickness [7–9]. We have demonstrated the scalability of the process by growing free-standing zinc-blende GaN layers up to 3-in. diameter. Thick zinc-blende GaN films were grown by PA-MBE on 2-in. GaAs (0 0 1) substrates and were removed from the GaAs substrate after the growth. We have used free-standing GaN wafers with thicknesses in the 30–100 μm range as substrates for further epitaxy of cubic GaN-based structures and devices. The side of the GaN crystal previously in contact with GaAs substrate was used as the epi-side surface for the zinc-blende GaN substrate fabrication. The surface is very smooth as measured by AFM and has an RMS roughness of ~0.5 nm.

* Corresponding author.
E-mail address: Sergei.Novikov@Nottingham.ac.uk (S.V. Novikov).

0022-0248/$ - see front matter © 2011 Elsevier B.V. All rights reserved.
doi:10.1016/j.jcrysgro.2011.12.028

The only potential disadvantage of using this side of free-standing zinc-blende GaN as the epi-side for the substrate fabrication is possible unintentional arsenic contamination on this side of the zinc-blende GaN bulk crystal. We have demonstrated both by secondary ion mass spectroscopy (SIMS) and by electron probe microanalysis (EPMA) that As incorporation is limited to the first few hundred nanometres of the layer and is due to initiation phase of the growth of zinc-blende material [10]. We have developed a process to remove this thin, lightly As contaminated, region of GaN using a chemical-mechanical polishing technique. We are able to maintain the mirror like surface after polishing with RMS values similar to that of the original surface. We have developed a procedure to cleave the wafers into the shape and size required for further processing to produce free-standing zinc-blende GaN substrates. The first zinc-blende GaN/InGaN LEDs have been demonstrated by our collaborators, using our zinc-blende GaN substrates [11].

In this paper we will describe the extension of our PA-MBE approach to the growth of free-standing zinc-blende and wurtzite $Al_xGa_{1-x}N$ bulk crystals.

2. Experimental details

Zinc-blende (cubic) and wurtzite (hexagonal) $Al_xGa_{1-x}N$ films were grown on GaAs substrates by plasma-assisted molecular beam epitaxy (PA-MBE) in a MOD-GENII system [7,8]. Two-in. diameter GaAs substrates were used. The active nitrogen for the growth of the group III-nitrides was provided by an HD25 RF activated plasma source. Prior to the growth of the $Al_xGa_{1-x}N$ layers, a GaAs buffer layer was grown on the GaAs substrate in order to improve the properties of the $Al_xGa_{1-x}N$ films. We have grown a thin GaN buffers before the growth of the $Al_xGa_{1-x}N$ layers of desired composition. All $Al_xGa_{1-x}N$ layers were grown under strongly group III-rich conditions in order to achieve the best structural quality layers. In the current study the $Al_xGa_{1-x}N$ layers were grown at temperatures of $\sim$680 °C and at a growth rate of $\sim$0.25 μm/hr.

We have grown $\sim$10 μm thick $Al_xGa_{1-x}N$ layers on GaAs substrates and subsequently removed the GaAs using a chemical etch (20 ml H_3PO_4 : 100 ml H_2O_2) in order to achieve free-standing $Al_xGa_{1-x}N$ wafers. From our previous experience with MBE growth of zinc-blende GaN [7–9], such a thickness is already sufficient to obtain free-standing GaN and $Al_xGa_{1-x}N$ layers without cracking and at the same time it does not require very long growth runs. To increase the thickness even further to 50–100 μm is merely a technical task as we have shown earlier [7–9]. Therefore, for this demonstration of the feasibility of the method, we have chosen to grow the majority of the bulk zinc-blende and wurtzite $Al_xGa_{1-x}N$ layers $\sim$10 μm thick.

From our experience of working with thin free-standing zinc-blende GaN layers [7–9], we know that $\sim$10 μm thick cubic $Al_xGa_{1-x}N$ layers will bow if they are removed from the glass. The extent of the bowing depends strongly on the thickness of the $Al_xGa_{1-x}N$ layer and possibly on the Al content. The $\sim$10 μm thick (Al)GaN layers are also very fragile and difficult to handle. Therefore, we have kept the bulk $Al_xGa_{1-x}N$ layers mounted on glass for further studies.

Samples were studied in-situ using reflection high-energy electron diffraction (RHEED) and after growth ex-situ measurements were performed using X-ray diffraction (XRD). To investigate the optical properties of free-standing $Al_xGa_{1-x}N$ layers we have studied photoluminescence (PL) and cathodoluminescence (CL). In PL we have used a quadrupled tuneable ps Ti:Sapphire laser operating at 190–330 nm. For CL we used an FEI Sirion 200 scanning electron microscope.

We have studied Al incorporation in the zinc-blende and wurtzite $Al_xGa_{1-x}N$ layers by secondary ion mass spectrometry (SIMS) using Cameca IMS-3 F and IMS-4 F systems and by electron probe microanalysis (EPMA) using a Cameca SX100 apparatus.

3. Results and discussion

3.1. Epitaxy of zinc-blende $Al_xGa_{1-x}N$

Zinc-blende $Al_xGa_{1-x}N$ films were grown on semi-insulating GaAs (0 0 1) substrates by PA-MBE using arsenic (As_2) as a surfactant to initiate the growth of cubic phase material [7–9]. We have developed MBE growth of thin ($\sim$1 μm) cubic $Al_xGa_{1-x}N$ layers for the complete Al composition range x from 0 up to close to 1. We have used $\sim$75 nm cubic GaN buffers to initiate the growth of the cubic phase. In order to sustain the cubic phase during the epitaxy it is crucial to maintain an excess of group III elements on the growth surface. It is well established that exposing a c-AlN surface to nitrogen flux leads to the formation of hexagonal AlN clusters [12,13]. We have used a new approach to maintain the excess of group III elements for the growth of $Al_xGa_{1-x}N$ layers for a wide Al composition range: namely the use of an excess Ga flux. The energy of the Al–N bond is significantly stronger than the energy of Ga–N bond. Therefore, we have observed preferential incorporation of Al into the $Al_xGa_{1-x}N$ layers from the Ga–Al liquid on the surface. This method allows us to sustain zinc-blende growth of $Al_xGa_{1-x}N$ layers over practically the whole Al composition range. The only disadvantage of this approach is the excess Ga present on the surface after growth and formation of Ga-rich droplets. However, these can be chemically removed after epitaxy and they will not be present on the side previously attached to GaAs.

We have observed a monotonic increase of the band gap of the zinc-blende $Al_xGa_{1-x}N$ layers with increasing Al content in both cathodoluminescence (CL) and photoluminescence (PL) studies. We have shown [14] that photoexcited electrons and holes in cubic $Al_xGa_{1-x}N$ layers at high Al content possess strong localisation at room temperature. As a result, the intensity of the near-band edge PL increases by more than 2 orders of magnitude in comparison with pure zinc-blende GaN.

Based on the results for these thin $Al_xGa_{1-x}N$ layers, we have developed MBE growth of bulk free-standing cubic $Al_xGa_{1-x}N$ layers with Al content x from 0 up to close to 1. Fig. 1a presents XRD data from a free-standing $Al_xGa_{1-x}N$ wafer with a composition of $x\sim$0.1 and a thickness of $\sim$10 μm. XRD demonstrates only a single peak at $\sim$40 degrees, which is the correct position of the peak for cubic $Al_xGa_{1-x}N$. In a 2θ-ω scan, the position of the main (0002) peak for hexagonal $Al_xGa_{1-x}N$ has a 2θ value of $\sim$35 degrees, which coincides precisely with the (1 1 1) peak for cubic $Al_xGa_{1-x}N$ at $\sim$35 degrees. There is no evidence for a peak at that position within experimental error as shown in Fig. 1a. However, this does not preclude the possibility of some hexagonal inclusions growing parallel to the [1 1 1] direction of the cubic $Al_xGa_{1-x}N$. This type of inclusion can only be detected using pole figures or reciprocal space maps looking at asymmetric peaks and we are working on a reliable method to quantify the relative fraction of any hexagonal inclusions using the integrated intensity of suitable reflections.

Even thicker free-standing zinc-blende $Al_xGa_{1-x}N$ layers, with thickness up to 75 μm and different AlN contents, have also been grown and they have confirmed that the results obtained on the 10 μm thick samples are representative of much thicker material.

We have studied Al incorporation in the layers using SIMS and EPMA. In the SIMS studies of the thin zinc-blende $Al_xGa_{1-x}N$ layers we were able to sputter through the $Al_xGa_{1-x}N$ layer into

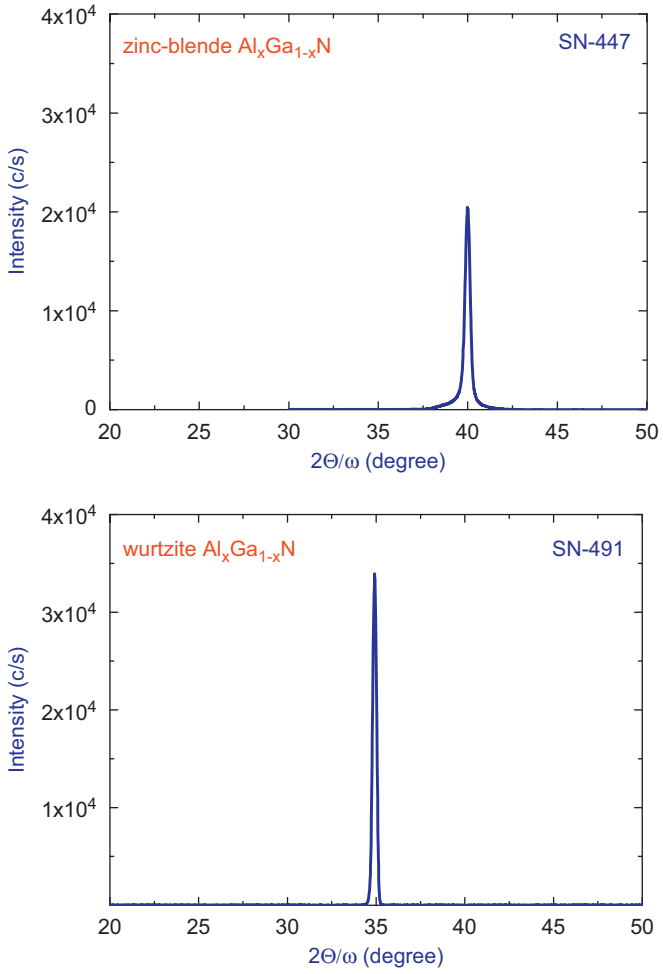

Fig. 1. A 2θ-ω XRD scan showing the 0002 peak at the centre of a ~10 μm thick 2-in. diameter bulk $Al_xGa_{1-x}N$ wafers: (a) zinc-blende $Al_xGa_{1-x}N$ layer with $x \sim 0.1$ and (b) wurtzite $Al_xGa_{1-x}N$ layer with $x \sim 0.3$.

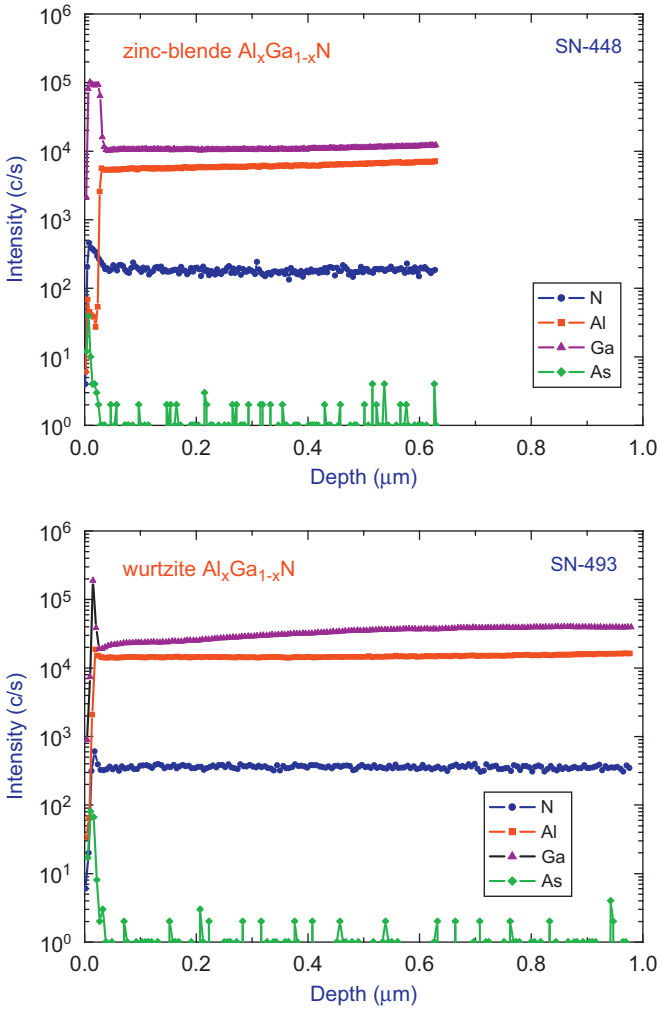

Fig. 2. SIMS profiles for Al, Ga, As and N at the centre of an $Al_xGa_{1-x}N$ layer on the side previously in contact with the GaAs substrate: (a) zinc-blende $Al_xGa_{1-x}N$ layer with $x \sim 0.5$ and (b) wurtzite $Al_xGa_{1-x}N$ layer with $x \sim 0.5$.

the GaAs substrate. For the thicker layers (~10 μm range), SIMS sputtering through the whole bulk of the layer is not viable. We have performed SIMS studies on both sides of the free-standing $Al_xGa_{1-x}N$ layers. Fig. 2a shows the Al, Ga, N and As distributions in $Al_xGa_{1-x}N$ crystal on the surface of an $Al_xGa_{1-x}N$ crystal previously attached to the GaAs substrate. The Al concentration in the $Al_xGa_{1-x}N$ layers is $x \sim 0.5$. The $Al_xGa_{1-x}N$ layer were grown on the top of a ~75 nm thick GaN buffer, which can be seen on the left part of the graph. The sputtering time was limited to ~15 min. We have observed a uniform distribution of Al, Ga and N within the bulk of $Al_xGa_{1-x}N$ layer. There is no significant As incorporation into the bulk of $Al_xGa_{1-x}N$ layer, which was confirmed by the As signal being at the background level of the SIMS system. Unfortunately, due to the lack of SIMS calibration standards for zinc-blende GaN we were not able to measure the exact concentrations of the matrix elements and other impurities. Fig. 2a show that the MBE method we have developed allows us to achieve the growth of bulk $Al_xGa_{1-x}N$ crystals with a constant composition.

In order to study the lateral distribution of the elements across the 2-in-diameter $Al_xGa_{1-x}N$ wafer, we have performed EPMA studies on the surface of the $Al_xGa_{1-x}N$ crystal previously attached to the GaAs substrate. Fig. 3a shows the lateral distribution of the Al content for two free-standing $Al_xGa_{1-x}N$ wafers with $x \sim 0.1$ and $x \sim 0.3$. We have measured the Al, Ga and N concentrations at several points along the radius of the 2 in. wafer by EPMA and present the Al distribution in the form of the cation ratio [Al]/([Al]+[Ga]), which minimises additional measurement errors from small variations in the N fraction. Fig. 3a confirms that we were able to achieve a uniform distribution of Al content across the diameter of the 2 in. $Al_xGa_{1-x}N$ wafer for the low Al content. However, with increasing Al concentration the distribution becomes less uniform, with the minimum Al content close to the centre of the wafer. We can attribute this effect to the strong dependence of the Al incorporation on the group III:N ratio during the MBE under Ga-rich conditions. It is well established in the MBE growth of hexagonal $Al_xGa_{1-x}N$ layers that under the Ga-rich conditions of the growth, the Al fraction increases with decreasing N flux due to preferential incorporation of the Al over Ga [15,16]. In our case we have slightly more N-rich conditions in the centre of the wafer. We are now investigating ways of minimising this effect.

3.2. Epitaxy of wurtzite $Al_xGa_{1-x}N$

Initially we have performed PA-MBE growth of thin (~1 μm) wurtzite $Al_xGa_{1-x}N$ layers on 2-in. diameter Si-doped (1 1 1)B GaAs substrates for Al compositions ranging from 0 up to 0.5. This substrate orientation was chosen in order to initiate the epitaxy of the hexagonal phase. We have grown ~50 nm wurtzite GaN buffers before the growth of the $Al_xGa_{1-x}N$ layers of any desired

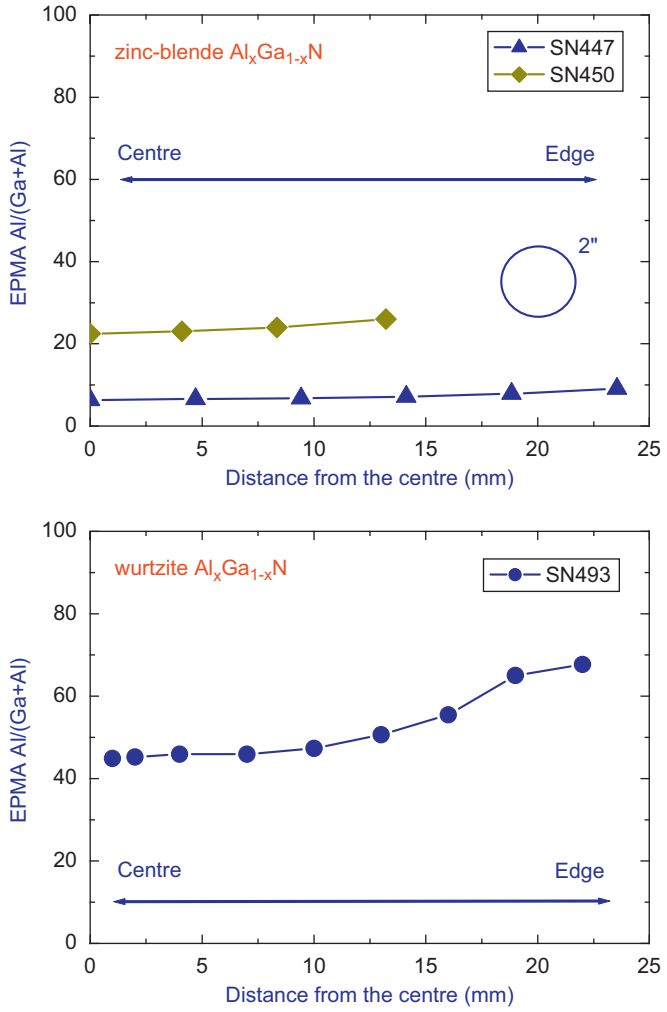

Fig. 3. EPMA data on the lateral distribution of Al on the surface of 2-in diameter $Al_xGa_{1-x}N$ layers mounted on glass, measured at 8 kV and 20 nA: (a) zinc-blende $Al_xGa_{1-x}N$ layers with $x\sim0.1$ and 0.3 and (b) wurtzite $Al_xGa_{1-x}N$ layer with $x\sim0.5$.

composition. As expected, in 2θ–ω XRD plots with increasing Al content in the layers we observed a gradual shift of the position of the $Al_xGa_{1-x}N$ XRD peak to higher angle. PL and CL studies have confirmed an increase of the band gap of $Al_xGa_{1-x}N$ layers with increasing Al content.

Based on these results we have grown ~10 μm thick wurtzite $Al_xGa_{1-x}N$ layers under similar growth conditions with x ranging from 0 up to 0.5. Fig. 1b shows a 2θ–ω XRD plot for a 10 μm thick free-standing wurtzite $Al_xGa_{1-x}N$. In XRD studies we have observed a single peak at ~35 degrees, which is the correct position for a wurtzite $Al_xGa_{1-x}N$ layer. Using Vegard's law, we can estimate the composition of the $Al_xGa_{1-x}N$ layer shown in Fig.1(b) to be $x\sim0.3$. The value of Al content in this $Al_xGa_{1-x}N$ layer was also confirmed later by EPMA measurements. As we have previously shown [17], from high resolution XRD scans we can estimate the zinc-blende fraction, which in this case was below our detection limit ($<0.1\%$). The intensity of the 35 degree peak is very strong with a full width at half maximum (FWHM) of only ~0.27 degrees. It is important to note that for the $Al_xGa_{1-x}N$ layer with a similar composition of $x\sim0.3$, but with a thickness of only ~0.5 μm the FWHM was similar. This data confirms that we are able to sustain the same reasonable structural quality of wurtzite $Al_xGa_{1-x}N$ layers whilst increasing it in thickness from the very thin layers up to ~10 μm. It is different from the growth of zinc-blende $Al_xGa_{1-x}N$ layers, where the initiation of hexagonal inclusions remains the constant problem with increase in the thickness. This is a very significant result, because it shows that MBE can be a viable method for the growth of bulk wurtzite $Al_xGa_{1-x}N$ crystals. In order to study in detail the changes in structural quality with sample thickness and Al composition, we have investigated reciprocal space maps and rocking curves for this series of samples. The XRD results for FWHM ω for free-standing 10 μm thick wurtzite $Al_xGa_{1-x}N$ layers are shown in Fig. 4. We have observed a gradual increase in FWHM ω and decrease in XRD peak intensity with increasing Al composition in $Al_xGa_{1-x}N$ layers from 0 to $x\sim0.5$. The intensity of the XRD peak is still strong and the FWHM ω is relatively narrow for all $Al_xGa_{1-x}N$ layers, which confirms that MBE can be used as a method for the growth of bulk wurtzite $Al_xGa_{1-x}N$ crystals for a wide range of the Al compositions.

We have studied depth uniformity of Al incorporation into the $Al_xGa_{1-x}N$ layers using SIMS. Fig. 2b shows SIMS profiles for Al, Ga, As and N at the centre of an $Al_xGa_{1-x}N$ layer with $x\sim0.5$ on the side previously in contact with the GaAs substrate. After sputtering through initial GaN layer and stabilizing of the sputtering conditions we have observed a uniform distribution of Al, Ga and N within the bulk of $Al_xGa_{1-x}N$ layers with different Al contents. There is no significant As incorporation into the bulk of $Al_xGa_{1-x}N$ layers, which was confirmed by the As signal being at the background level of the SIMS system.

In order to study the lateral distribution of the elements across the 2-in. diameter $Al_xGa_{1-x}N$ wafer, we have performed EPMA studies on the surface of the $Al_xGa_{1-x}N$ crystal previously attached to the GaAs substrate. Fig. 3b shows the lateral distribution of the Al content for the ~10 μm thick free-standing $Al_xGa_{1-x}N$ wafer with $x\sim0.5$. Figure confirms that we were able to achieve a uniform distribution of Al content across the diameter for the central part (~35 mm in diameter) of the 2-in. $Al_xGa_{1-x}N$ wafer. However, close to the edge of the wafer the Al distribution becomes less uniform, with the maximum Al content close to the edge of the wafer. This is similar to EPMA results for zinc-blende $Al_xGa_{1-x}N$ wafer (Fig. 3a) and can be attributed to the strong dependence of the Al incorporation on the group III:N ratio during MBE as discussed above. In our case we have slightly more group III-rich conditions at the edges of the 2-in. wafer due to temperature non-uniformity. In order to minimise this effect we will optimise the thickness of the PBN backing plates used in our MBE substrate holders.

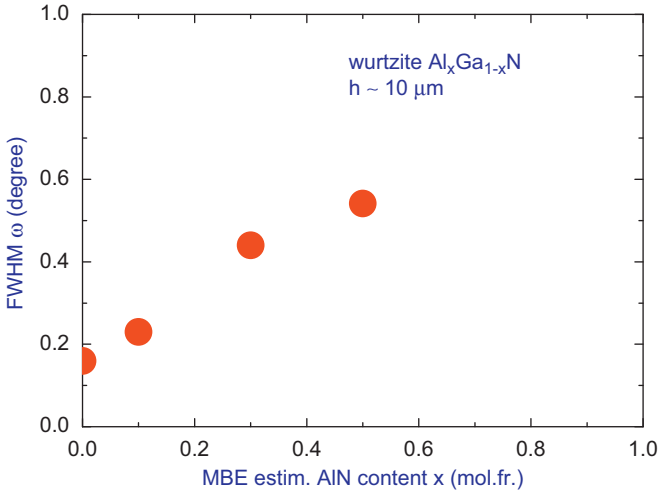

Fig. 4. FWHM of ω for 10 μm thick wurtzite $Al_xGa_{1-x}N$ layers with the different Al content.

The fact that uniform free-standing ternary zinc-blende and wurtzite $Al_xGa_{1-x}N$ wafers with a thickness up to 10 μm can be grown by MBE is very important for the potential future production of wurtzite $Al_xGa_{1-x}N$ substrates by MBE of any desired composition. We have already shown that free-standing zinc-blende GaN wafers with thicknesses in the 30–100 μm range can be used as substrates for further epitaxy of cubic GaN-based device structures [11]. We have also recently used the PA-MBE technique to produce such free-standing layers of zinc-blende GaN up to 100 μm in thickness [9], so increasing the thickness is merely a technical task for MBE. Therefore, the first results presented above on the growth of uniform ternary zinc-blende and wurtzite $Al_xGa_{1-x}N$ wafers allow us to conclude that MBE may be a viable method for the production of zinc-blende and wurtzite $Al_xGa_{1-x}N$ substrates.

4. Summary and conclusions

We have developed a process for the growth of 10 μm thick bulk, free-standing, zinc-blende and wurtzite GaN and $Al_xGa_{1-x}N$ layers by PA-MBE. The quality of the bulk $Al_xGa_{1-x}N$ layers has been confirmed by XRD, CL and PL studies. The uniform lateral Al distribution in the bulk $Al_xGa_{1-x}N$ layers has been confirmed by EPMA and Al depth uniformity has been confirmed by SIMS. The fact that free-standing zinc-blende and wurtzite $Al_xGa_{1-x}N$ wafers can be grown by MBE opens the possibility of the future production of $Al_xGa_{1-x}N$ substrates for further epitaxy of AlGaN-based device structures.

Acknowledgements

This work was undertaken with support from the EPSRC (EP/I004203/1, EP/I00467X/1, EP/G046867/1 and EP/G030634/1). We want to acknowledge D. E. Sykes, A. Chew and M. Petty from Loughborough Surface Analysis Ltd for SIMS measurements and discussions of results.

References

[1] J.H. Edgar, S. Strite, I. Akasaki, H. Amano, C. Wetzel (Eds.), Gallium Nitride and Related Semiconductors, INSPEC, Stevenage, ISBN 0 85296 953 8, 1999.
[2] I. Grzegory, S. Krukowski, M. Leszczynski, P. Perlin, T. Suski, S. Porowski, Acta Physica Polonica A 100 (2001) 57.
[3] P. Geiser, J. Jun, S.M. Kazakov, P. Wägli, J. Karpinski, B. Batlogg, L. Klemm, Applied Physics Letters 86 (2005) 081908.
[4] A. Belousov, S. Katrych, J. Jun, J. Zhang, D. Gunther, R. Sobolewski, J. Karpinski, B. Batlogg, Journal of Crystal Growth 311 (2009) 3971.
[5] 〈www.compoundsemiconductor.net〉; Compound Semiconductor 16 (2010) 12.
[6] V. Yu., V.A. Melnik, K.V. Soukhoveev, V.A. Tsvetkov, M.R.S. Dmitriev, Symposia Proceedings 764 (2003) 363.
[7] S.V. Novikov, N.M. Stanton, R.P. Campion, R.D. Morris, H.L. Geen, C.T. Foxon, A.J. Kent, Semiconductor Science and Technology 23 (2008) 015018.
[8] S.V. Novikov, N.M. Stanton, R.P. Campion, C.T. Foxon, A.J. Kent, Journal of Crystal Growth 310 (2008) 3964.
[9] S.V. Novikov, N. Zainal, A.V. Akimov, C.R. Staddon, A.J. Kent, C.T. Foxon, Journal of Vacuum Science and Technology B 28 (2010) C3B1.
[10] S.V. Novikov, N. Zainal, C.T. Foxon, A.J. Kent, F. Luckert, P.R. Edwards, R.W. Martin, Physica Status Solidi C 7 (2010) 2033.
[11] S.V. Novikov, N. Zainal, A.V. Akimov, C.R. Staddon, C.T. Foxon, A.J. Kent, D.P. Nicholls, S.E. Hooper, Proceedings of ICNS-8 P4 (2009) 494.
[12] T. Schupp, K. Lishka, D.J. As, Journal of Crystal Growth 312 (2010) 1500.
[13] M. Roppischer, R. Goldhahn, G. Rossbach, P. Schley, C. Cobet, N. Esser, T. Schupp, K. Lishka, D.J. As, Journal of Applied Physics 106 (2009) 076104.
[14] R.E.L. Powell, S.V. Novikov, F. Luckert, P.R. Edwards, A.V. Akimov, C.T. Foxon, R.W. Martin, A.J. Kent, J. Appl. Phys 110 (2011) 063517.
[15] L. He, M.A. Reshchikov, F. Yun, D. Huang, T. King, H. Morkoc, Applied Physics Letters 81 (2002) 2178.
[16] E. Iliopoulos, T.D. Moustakas, Applied Physics Letters 81 (2002) 295.
[17] T. Li, C.R. Staddon, S.V. Novikov, P.F. Fewster, A. Widdowson, N.L. Andrew, P. Kidd, I. Harrison, A. Winser, Y. Liao, C.T. Foxon, Journal of Crystal Growth 235 (2002) 103.